Chapter 5

Exploring the ability of genetically modified rhizobia to produce nanoparticles to combat heavy metal stress.

5.1 Introduction

5.1.1 Heavy metal bioremediation by microorganisms

The development of novel technologies and approaches to combat the issue of heavy metal contamination using environmentally friendly techniques, broadly categorised as bioremediation, is the focus of research on a global scale. Heavy metals from the soil and water are bioremediated by microorganisms such fungi, bacteria, and viruses. To combat the presence of heavy metals in their environment, bacteria have a variety of methods including extracellular barriers, efflux pumps, intracellular/extracellular sequestration, and reduction of metal ions.[1] Many genera of soil bacteria and Plant growth promoting bacteria (PGPB) such as Mesorhizobium, Sinorhizobium and Bradyrhizobium have shown their ability to tolerate the presence of heavy metals like Cd, Co, Fe, Ni, Zn and Cu [2]in their environment. The remarkable ability of bacteria to reduce the metal ions thus converting them into less toxic forms is the best candidate for metal nanoparticle synthesis.[3]

5.1.2 Biosynthesis of nanoparticles by microorganisms

Wild type as well as genetically modified bacteria have a potential to produce varieties of metal nanoparticles in *invitro* conditions.[3,4] Also, *Escherichia coli* (MTCC10312) showed extracellular[5] production of cadmium sulphide quantum dots. Also, a cyanobacteria *Oscillatoria limnetica* has been shown to produce silver nanoparticles.[6] Not only wild type but genetically modified bacteria could be a good tool to manufacture nanoparticles in *invitro* conditions. It was reported that genetically modified *Escherichia coli* over expressing glutathione synthetase showed augmented biosynthesis of cadmium sulphide nanoparticles. [7]Also, *Escherichia coli* expressing *Candida albicans* Metallothionine gene and *Rhizobium tropici* Phytochelatin synthetase gene showed enhanced production of silver nanoparticles[8] and selenium nanoparticles[9] respectively. Biogenic nanomaterial have unique physical and chemical properties and they are used in varieties of industries such as electronic, chemical, photonics, energy and medical.[10] It is clear that microbe-based nanoparticles production could be cheaper and environment friendly. Also, their unique properties allow its traditional as well as novel application in a wide spectrum of Industries.[11] Genetically modified *Escherichia coli* strain coexpressing Metallothionine and Phytochelatin synthetase been reported to produce 33 inorganic nanoparticles (20 single element and 13 multi-element), [12] which is way more than capacity of a synthetic reaction to produce that many inorganic nanoparticles in a single reaction. Additionally, the ease to genetically manipulate the microbes makes it a best

candidate for enhanced production of nanoparticles in a way which consumes very less amount of energy thus contributing less in carbon foot print addition to our environment. Phytochelatin as well as Metallothionine have been extensively expressed/coexpressed/overexpressed for biosynthesis of nanoparticles such as *PCS* and *ghs1* genes of *Schizosaccharomyces pombe* overexpressed in *E. coli* for CdS nanoparticles synthesis.[13] Also enhanced production of glutathione by *Escherichia coli* showed intracellular production of CdTe quantum dots.[14] The probable mechanism of thiol containing proteins, amino acids and short peptides is to from metal thiolate conjugate with the heavy metals, which can be explained by nRSH + Mn+ ↔ (RS)n-M + nH+ equation.[15]

5.1.3 Rationale behind the objective

We have shown that the PGPR's used in this study can produce glutathione and the heterologous expression of *E. coli* DH10B *ybdk* gene in the rhizobium can accumulate more glutathione in GMO bacteria compared to its wildtype counterpart (Chapter 3). These GMO bacteria has also been successful in alleviating heavy metal induced stress in fenugreek seedlings compare wild type bacteria (Chapter 4). Various PGPR's including rhizobium are capable of biosynthesizing nanoparticles due to their ability to produce glutathione, metallothionine and phytochelatins (5.1.2). This study compares the ability of GMO and wild type bacteria to produce heavy metal nanoparticles. We hypothesized that; various metal sequestration mechanisms present in bacteria (5.1.1) and enhanced levels of glutathione will enable them to sequester heavy metals and trap them, which will reduce the availability of heavy metals for plants, thus alleviating the heavy metal induced stress. Therefore, this chapter describes and discusses the invitro experiments which can prove the ability of GMO and WT bacteria to biosynthesize nanoparticles.

5.2 Materials and methods

5.2.1 Biosynthesis of Cadmium sulphide nanoparticles and glutathione estimation

Bacteria M1; *Pseudomonas fluorescence* (NAIMCC B-00342), M2; *Sinorhizobium fredii* NGR 234, M3; *Sinorhizobium fredii* NGR 234 (pPAT), M4; *Sinorhizobium meliloti* (NIAMCC B-00836), M5; *Sinorhizobium meliloti* (NIAMCC B-00836) (pPAT) were grown in 100 ml flask containing 50 ml nutrient media (King's B for *Pseudomonas* and YEM for rhizobia) in an incubator shaker at 120 rpm and 28 °C for more than 48 hours. Cell suspension was centrifuged, cell biomass was discarded and the supernatant was collected for biosynthesis of cadmium

sulphide nanoparticles. 1 ml supernatant was aliquoted for glutathione estimation. The supernatant was treated with 20% w/v TCA solution (final concentration of TCA is 5% in the mixture) to precipitate all the proteins. Precipitates were removed by centrifugation at 13000 g for 15 minutes and supernatant was collected (whole process was done in dark condition at 0 °C) and stored at -80 °C for glutathione analysis. Glutathione was estimated from the supernatant by a colorimetric method which measures GSH before and after the reduction of GSSG to GSH by $NaBH_4$.[16] And for biosynthesis of nanoparticles, Cadmium chloride (0.25 M) and sodium sulphide (0.25 M) in 1:1 ratio was allowed to react in a separate flask, which forms an orange-yellow precipitates of Cadmium sulphide immediately. Equal volume (50 ml) of bacterial supernatant and cadmium sulphide suspension were allowed to react in a flask which was heated in a water bath at 60 °C for 10 minutes until the formation of fluffy orange yellow deposits at the bottom of flask, which indicated the formation of nanoparticles. The suspension was allowed to cool down and was incubated at room temperature for 14 hours and was observed for the formation of coalescent orange-yellow crystals. The crystals accumulated at the bottom were collected by discarding the suspension. The crystals were washed with acetone followed by sterile distilled water and air dried at 45 °C. They were stored at 4 °C for further use.[5]

5.2.2 Characterization of cadmium sulphide nanoparticles

First step of the characterization was to study the morphology of the nanoparticles, which was done by observing the nanoparticles crystals under the scanning electron microscope (Sigma VP SEM/Carl Zeiss NTS) and the micrographs were recorded.[5,17] FTIR spectrometry was performed by Bruker Alpha 2 spectrophotometer within the infrared range of 500- 3500 cm^{-1}, to have a better understanding of the functional groups attached to the nanoparticles.[18] Finally powder XRD was performed by XPERT PRO XRD machine to get a clear cut understanding about its crystalline structure. The intensities were recorded in a range of 10-80 ° 2θ angle.[5]

5.3 Results and Discussion

5.3.1 Glutathione estimation from supernatant

Bacteria M1; *Pseudomonas fluorescence* (NAIMCC B-00342), M2; *Sinorhizobium fredii* NGR 234, M3; *Sinorhizobium fredii* NGR 234 (pPAT), M4; *Sinorhizobium meliloti* (NIAMCC B-00836), M5; *Sinorhizobium meliloti* (NIAMCC B-00836) (pPAT) were able to excrete glutathione after 48 hours of growth in the liquid media, as shown in Table 5. M5 was able to excrete highest levels of glutathione after 48 hours, followed by M3, M4, M2 and M1 in decreasing order. The amount of glutathione excreted depends upon the bacterial species, its growth rate in a particular medium and growth conditions. It was observed that M3 (GMO) secreted 23 folds more glutathione compared to M2 (Wild type counterpart), while M5 (GMO) secreted 19.80 folds more glutathione compared to M4 (Wild type counterpart). Under normal conditions intracellular GSH can get converted to GSSG, which is a reversible enzymatic reaction. Intracellular GSH/GSSG ratio is always high in an actively growing cell, [19] while it is low in dying/stationary phase. This experiment summarizes the levels of extracellular glutathione. It was observed that the amount of the oxidized glutathione was significantly higher than reduced glutathione for M1-M5, which could be due to an absence of glutathione reductase enzyme,[20] as it is present inside the bacteria [21] and not in the growth media. Estimation of glutathione is performed from the growth media in the stationary phase (< 48 hr). It is known that bacteria in stationary phase produces toxin and ROS which significantly raises the oxidative stress.[22] Besides this the culture volume and vessel also contribute to the oxidative stress.[23] Excess oxidative stress might have converted entire secreted GSH to GSSG [24] in the media, and it is also known that extracellular glutathione is very important for neutralizing potential toxic electrophiles[25] and ROS generated in the growth media. In growing aerobic culture GSH is subjected to constant transmembrane circulation between the cells and the medium.[25] But in the late stationary phase cells change its shape and transport is affected as the membrane fluidity also reduces, which could be the reason behind high extracellular GSSG compared to GSH. [22] But overall, the concentration glutathione has been significantly high in the media of M3 and M5, which infers to the successful heterologous expression of *ybdK* gene in rhizobia. Besides this it is also reported that, *L. lactis* containing plasmid with gshA and gshB genes was reported to synthesize 140 mM glutathione and these results are the explanation to our results which reports high glutathione levels on transformation of rhizobia with *ybdK* gene, which has a similar function as gshA gene.

Table 5.1 Estimation of extracellular glutathione from nutrient media after 48 hours. Data represents mean ± SD (n=3), and p<0.05 were considered to be statistically significant.

Organism	Corresponding OD_{600} at 50 hr	Total glutathione (mM)	Oxidized glutathione (mM)	Reduced glutathione (mM)
M1	0.75	3.42 ± 0.39	2.15 ± 0.22	1.27 ± 0.37
M2	1.28	4.07 ± 0.001	3.3 ± 0.03	0.74 ± 0.02
M3	1.25	94.2 ± 0.03	93.8 ± 0.03	0.38 ± 0.02
M4	1.40	5.12 ± 0.30	3.50 ± 0.42	1.62 ± 0.15
M5	1.47	101.39 ± 4.93	100.37 ± 4.98	1.01 ± 0.35

5.3.2 Cadmium sulphide (CdS) nanoparticles biosynthesis

In the first step of reaction the fluffy cadmium sulphide precipitates are formed (5.2.1), and in the second step bacterial supernatant is mixed in it and heated at 60 °C for 10 minutes. Bacterial supernatant has carbohydrates, amino acids, proteins and other toxins released by the bacteria. Besides this it also contained more oxidized glutathione (GSSG) compared to the reduced glutathione (GSH). Owing to their surfactant like properties and the additional heat (60 °C,10 minutes) it dispersed the agglomerated CdS precipitates into very small particles on mixing with supernatant. Cadmium sulphide nanoparticles are known to possess an excellent photoreduction capability which can donate electrons when irradiated with light and reduce the oxidized compound. [26,27] This is known as a photocatalytic property and only CdS nanoparticles are capable of photoexcitation in a visible light [28] as the band gap energy of bulk CdS is around 2.4eV, which corresponds to the wavelength of 516 nm (i.e., visible range). Although all this depends on the particle size. Cadmium sulphide particles on coming in contact with GSSG might have reduced it to GSH as the reaction was happening in a glass beaker in an aerobic condition under the light and heated in water bath at 60 °C for 10 minutes. As the turnover number of the CdS nanoparticles were estimated around 47500 in a study,[26] we can postulate that a very small number of CdS particles would have reduced very high concentration of GSSG and other disulphide bond bearing compounds present in the supernatant on light irradiation. Following the formation of reduced glutathione (GSH), it would have capped CdS particles, stabilized it, and formed the nanoparticles. [29] There could be multiple possible explanations behind the formation of stabilized crystals (quantum

dots/nanoparticles) in this reaction, but this is our probable explanation. Nano particles deposited at the bottom of the beaker (Figure 5.1) were collected by carefully by discarding the supernatant followed by their washing and weighing. Total mass of nanoparticles collected after the reaction is mentioned in Table 5.2.

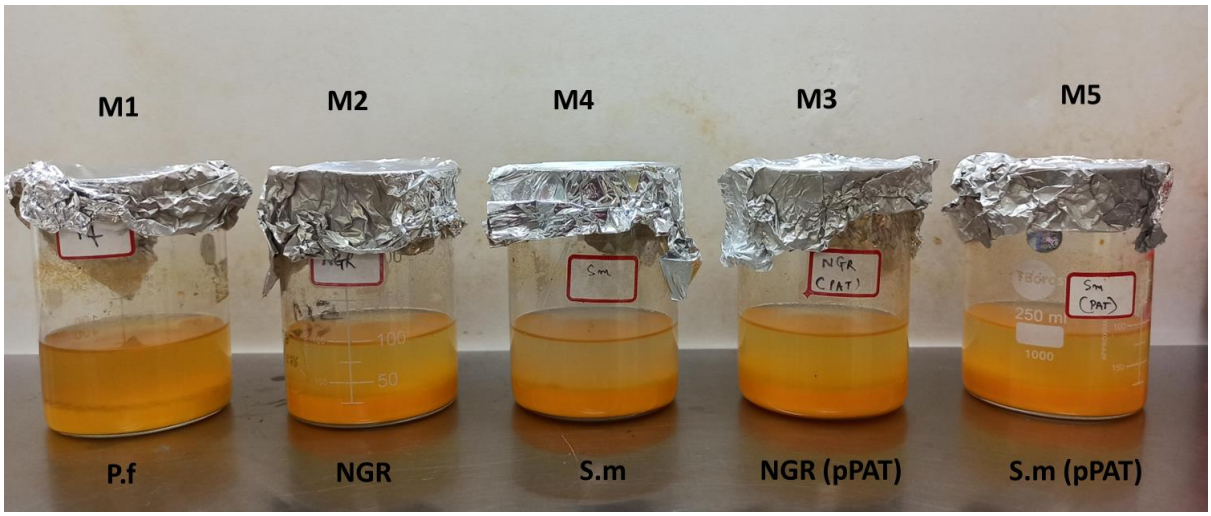

Figure 5.1 Biosynthesized nanoparticles deposited at the bottom of the beaker.

Table 5.2 Mass of cadmium sulphide crystals formed from 50 ml supernatant. Data represents mean ± SD (n=3), and $p<0.05$ were considered to be statistically significant.

Organism	Weight of nanoparticles (g)
M1	2.037 ± 0.006
M2	2.009 ± 0.001
M3	2.059 ± 0.001
M4	2.027 ± 0.004
M5	2.183 ± 0.031

It was observed that M3 produced 2.42% more CdS nanoparticles compared to M2 while M5 produced 7.15% more CdS nanoparticles compared to M4. Overall M5 produced highest number of nanoparticles followed by M3, M1, M4 and M2 in decreasing order (Table 5.2).

5.3.3. Characterization of Cadmium sulphide nanoparticles

It was observed that the nanoparticles produced by GMO rhizobium were darker compared to the nanoparticles produced by wildtype rhizobium (Figure 5.2). In a study it was observed that the CdS nanoparticles with glutathione/thiol capping appeared darker in colour compared to the uncapped CdS nanoparticles.[30]

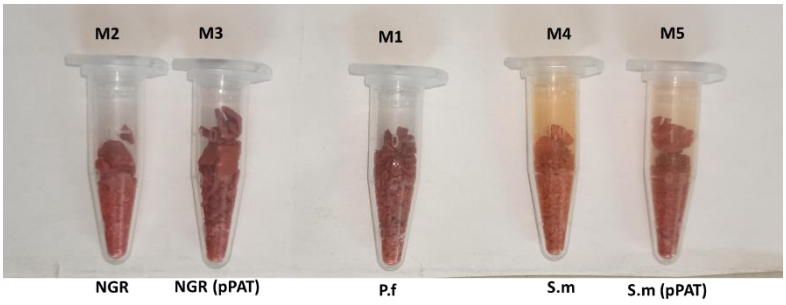

Figure 5.2 Nanoparticles collected after airdrying process

These results are in accordance to our findings where the nanoparticles produced by M3 and M5 are darked than the nanoparticles produced by M2 and M4 respectively, which correlates with the amount of glutathione excreted by GMO rhizobium and its counterpart wildtype rhizobium (Table 5.1). GMO rhizobium secreted more glutathione outside thus were able to produce more nanoparticles and consecutively their nanoparticles were darker in colour compared to the nanoparticles produced by WT rhizobium (Figure 5.1).

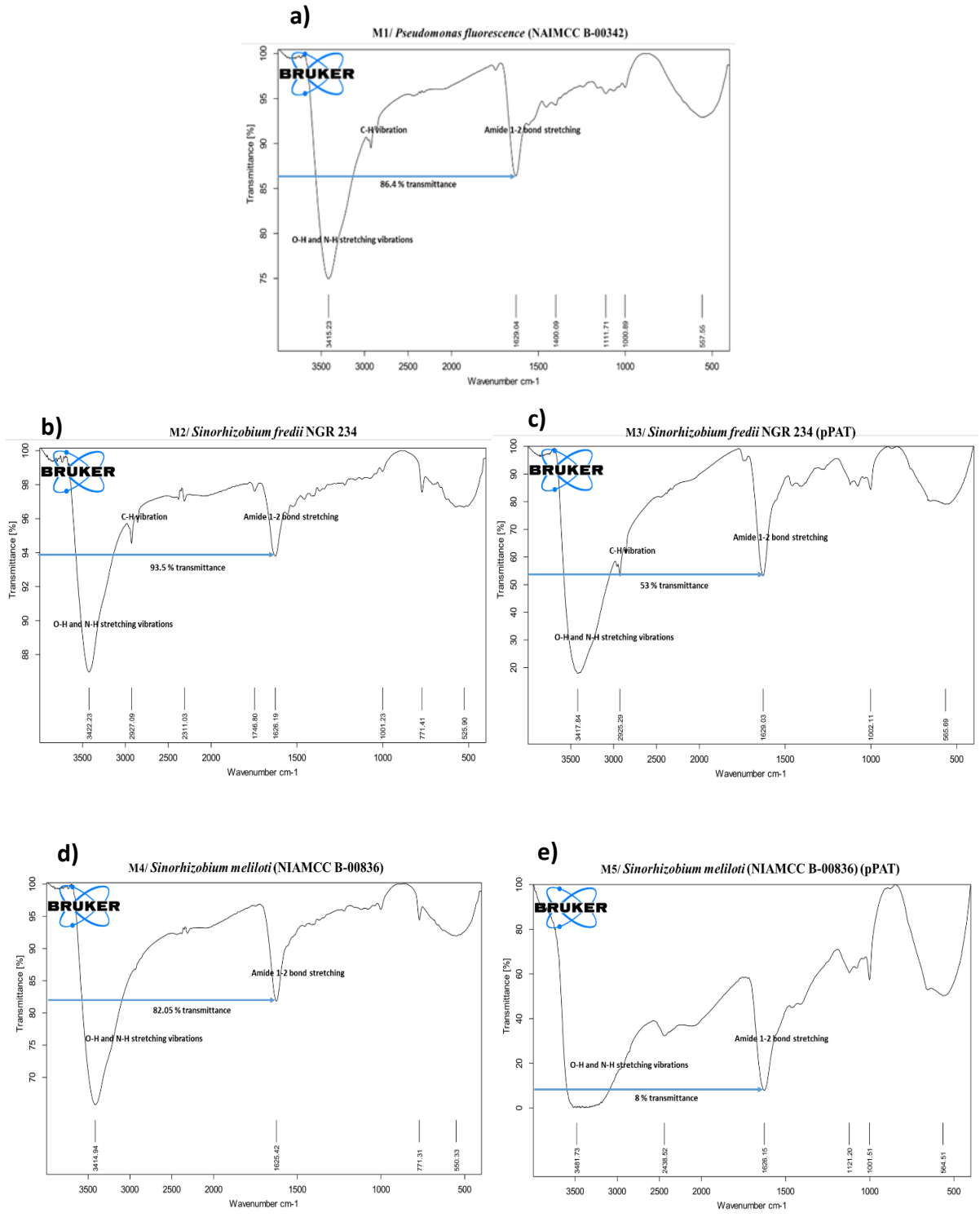

Figure 5.3 FTIR of CdS nanoparticles produced by a) M1 b) M2 c) M3 d) M4 e) M5 bacteria to analyse the molecules attached to its surface.

FTIR was performed to get an idea about the functional groups of the molecules attached to the surface of nanoparticles, to confirm the presence of glutathione on them (Figure 5.3.a-e). The FTIR analysis detected multiple transmittance peaks in the range of 3500 cm^{-1} to 500 cm^{-1} as shown in Figure 5.3. From the figure it is evident that in all the samples two prominent peaks are obtained in the range of 1600-1700 cm^{-1} and 3200-3700 cm^{-1}. The former range corresponds to the stretching vibration of the C=O bond and the N-H bond in the amide functional group of glutathione and other protein. Therefore, the peak observed around 1629 cm^{-1} is likely an amide I band.[31] The broad and intense peak in the range of 3200-3700 cm^{-1} could be the combination of two ranges, which includes amide A band [32] which has a range of about 3200-3400 cm^{-1} in which the N-H stretching vibrations have a primary contribution and another range is of about 3300-3700 cm^{-1} which corresponds to the O-H stretching vibrations. Both peaks (amide I band and amide A band) indicates the characteristic functional groups of glutathione,[33] which indicated the presence of glutathione in the sample. Only the peak around 2600 cm^{-1} (represents SH stretch [33]) was missing. This indicates that glutathione has conjugated with CdS nanoparticles by thiol group. Both GMO and wild type rhizobia synthesized and secreted glutathione in the growth media (Table 5.1). It was observed that the GMO rhizobium which secreted more glutathione showed a decrease in transmittance of amid I band in the FTIR spectra compared to compared to the FTIR spectra of the wild type rhizobium. The decrease in the transmittance correlates with the increase in the concentration of the functional group. This implies that more glutathione has surrounded/ capped CdS nanoparticles produced by GMO rhizobium in comparison to the CdS nanoparticles produced by wild type rhizobium. Amide I band in the FTIR spectra of CdS NPs produced by M3 (Figure 5.3.c) showed 53 % transmittance, while M2 (Figure 5.3.b) showed 93.5 % transmittance and the amide I band in the FTIIR spectra of CdS NPs produced by M5 (Figure 5.3.e) showed 8% transmittance, while M4 (Figure 5.3.d) showed 82.05 % transmittance. This proves that the rhizobium containing *ybdK* gene were able to synthesize more glutathione and secrete it out in the media. Thus, the rhizobium capable of secreting more glutathione is capable of making more nanoparticles and stabilizing them. In the entire study *P. fluorescens* is used as a positive control because this is the most common bacteria used in the majority of PGPR formulations. [34]

Visual examination of the SEM micrographs of the CdS nanoparticles produced by different bacteria revealed that the nanoparticles were in aggregates and they displayed variety of shapes (Figure 5.4.a-e). Nanoparticles produced by GMO rhizobium (M5 and M3) were smaller (i.e., smaller aggregates) compared to nanoparticles produced by wild type rhizobia (M4 and M2).

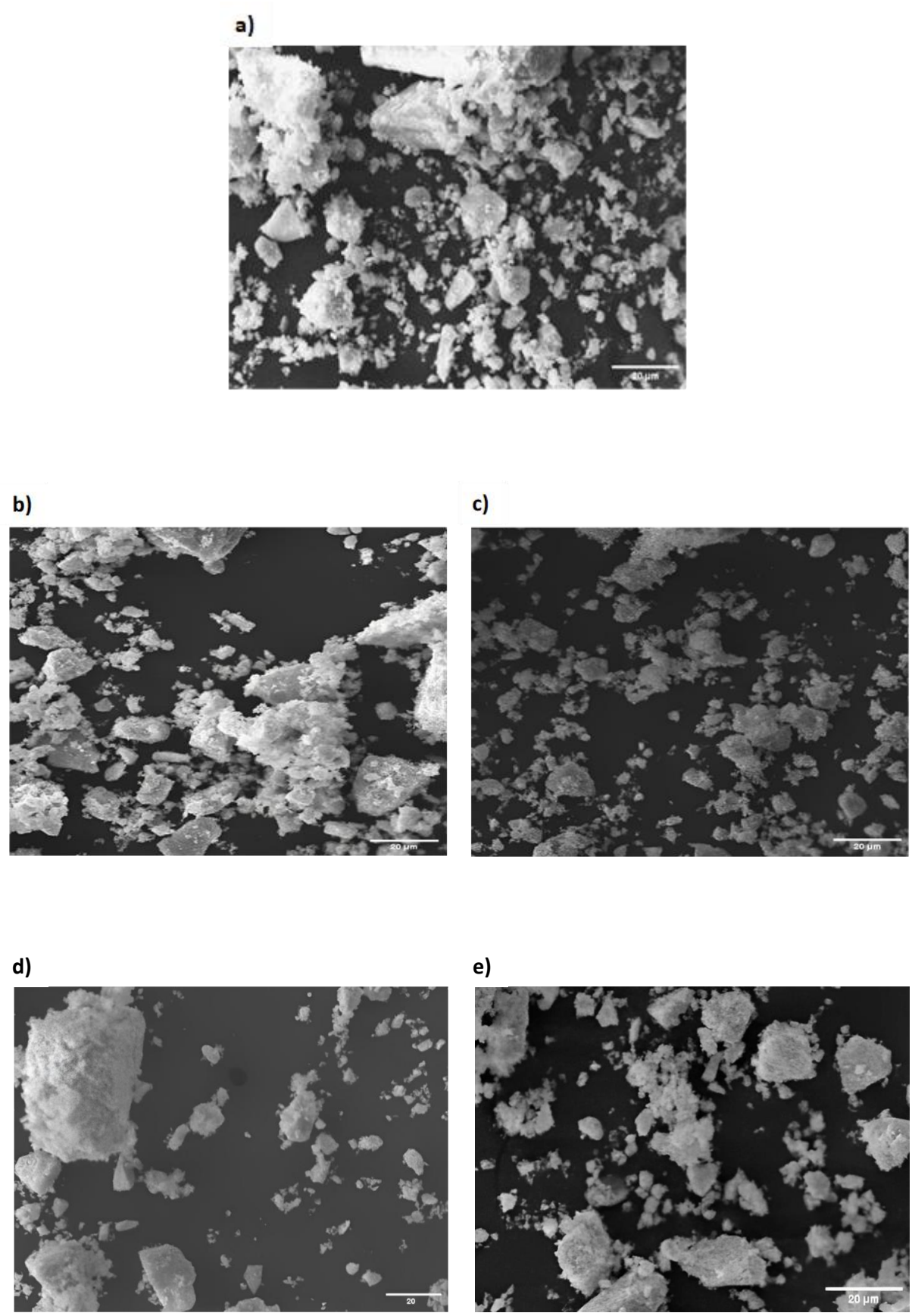

Figure 5.4) SEM analysis of the CdS nanoparticles produced by a) M1 b) M2 c) M3 d) M4 e) M5

Average size of aggregated nanoparticles produced by M5 was 626 nm, while the nanoparticle aggregates produced by M4 was 846 nm. Similarly, for M3 it was 343nm and for M2 it was 909 nm. M1 was used as a positive control in our study. The average size of nanoparticle aggregate produced by M1 was 909.86 nm. Our results were in accordance to the results obtained by a study where *E. coli* growth medium was used to synthesis of CdS nanoparticles.[5] Previous studies reported that the microorganisms capable of producing more glutathione[7] or phytochelatins [35] were able to produce relatively dispersed and smaller nanoparticles with tiny aggregates. Similar observations were recorded in this study. As shown in the Figure 5.4, M3 and M5 nanoparticle aggregates (Figure 5.4.c and 5.4.e) were smaller compared to the nanoparticles produced by M2 and M4 (Figure 5.4.b and 5.4.d) respectively. This experiment proves that the PGPR used in the study are capable of invitro production of CdS nanoparticles and this also proves that the rhizobium containing *ybdK* gene were able to synthesize more glutathione and secrete it out in the media.

For further confirmation of nanoparticles, XRD analysis was carried out which gave a proper understanding about the phase of nanoparticles. As shown in Figure 5.5.a - 5.5.e, the XRD pattern showed prominent peaks at 2θ values of 26°, 44° and 52° which corresponds to the reflection planes (111), (220) and (311) respectively, that indicates the cubic phase of the nanoparticles. The diffractogram of the sample reveals that all the peaks are in good agreement with the Joint committee on powder diffraction standard (JCPDS) data belonging to cubic CdS structure.[36–41]XRD data suggests that the material synthesized by the supernatant of bacteria are nanoparticles.

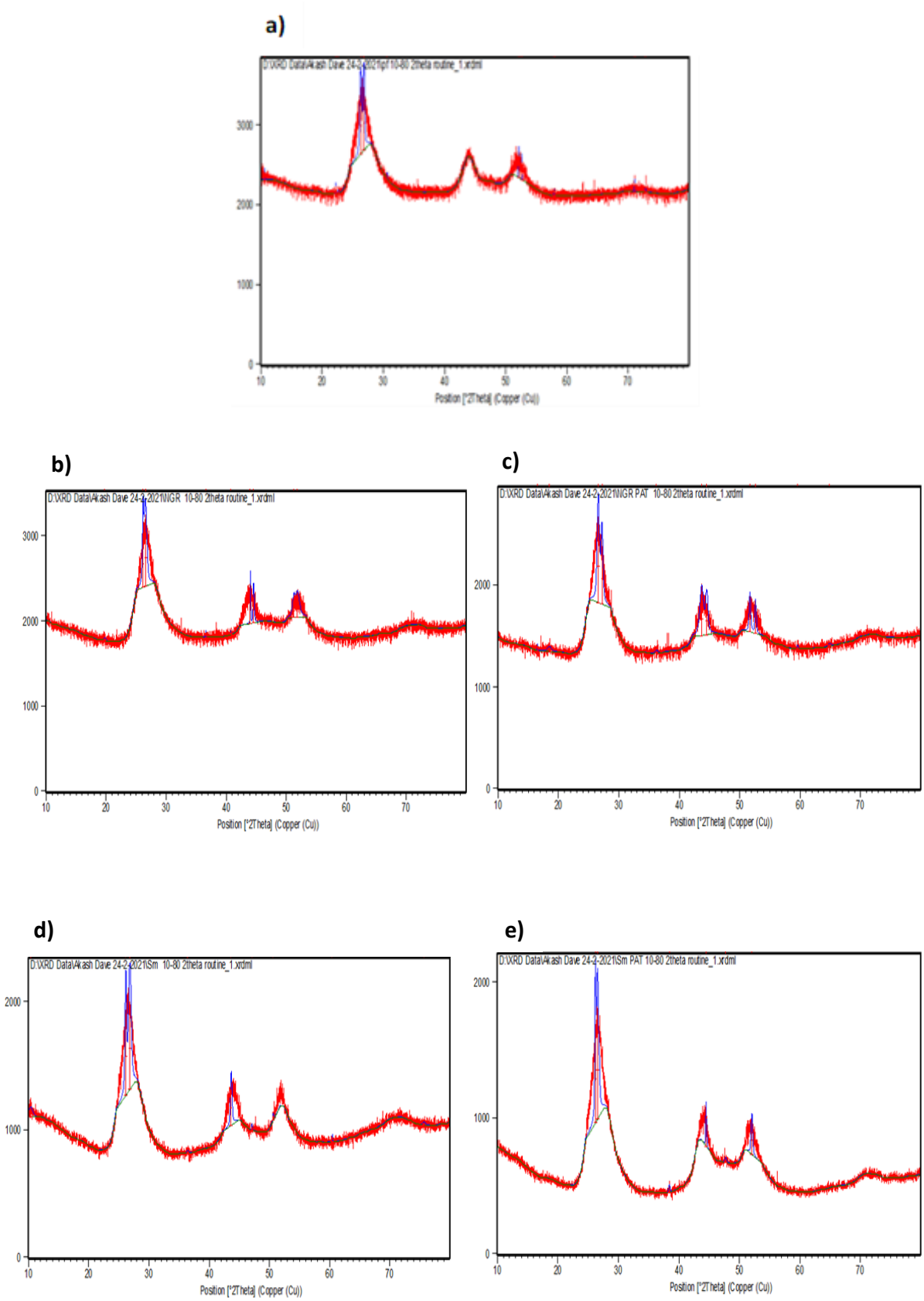

Figure 5.5) XRD analysis of the CdS nanoparticles produced by a) M1 b) M2 c) M3 d) M4 e) M5

5.4 Conclusion

Cloning *E. coli ybdK* gene in rhizobium enables it to secrete more glutathione compared to its wildtype counterparts. The high glutathione levels helped GMO rhizobia to synthesize slightly more nanoparticles which were in smaller aggregates compared to the wild type. Summing this conclusion in an agricultural perspective, we can say that the GMO rhizobia will secret more glutathione compared to the wildtype rhizobia in soil. More glutathione in soil could neutralize more cadmium (heavy metal pollution). Smaller CdS aggregates produced by bacteria provide them higher surface to volume ration which ultimately increase the chances for nanoparticles to get modified by other microorganisms present in rhizosphere. This would facilitate the clearing and detoxification of nanoparticles.

5.5 References

1. Nanda M, Kumar V, Sharma DK. Multimetal tolerance mechanisms in bacteria: The resistance strategies acquired by bacteria that can be exploited to 'clean-up' heavy metal contaminants from water. *Aquatic Toxicology*. 2019;212:1-10. doi:10.1016/j.aquatox.2019.04.011

2. Fagorzi C, Checcucci A, Dicenzo GC, et al. Harnessing rhizobia to improve heavy-metal phytoremediation by legumes. *Genes (Basel)*. 2018;9(11). doi:10.3390/genes9110542

3. Iravani S. Bacteria in Nanoparticle Synthesis: Current Status and Future Prospects. *Int Sch Res Notices*. 2014;2014:1-18. doi:10.1155/2014/359316

4. Hari S. Biosynthesis of nanoparticles from microorganisms. *Res J Pharm Technol*. 2020;13(4):2022-2026. doi:10.5958/0974-360X.2020.00364.9

5. Shivashankarappa A, Sanjay KR. Escherichia coli-based synthesis of cadmium sulfide nanoparticles, characterization, antimicrobial and cytotoxicity studies. *Brazilian Journal of Microbiology*. 2020;51(3):939-948. doi:10.1007/s42770-020-00238-9

6. Hamouda RA, Hussein MH, Abo-elmagd RA, Bawazir SS. Synthesis and biological characterization of silver nanoparticles derived from the cyanobacterium Oscillatoria limnetica. *Sci Rep*. 2019;9(1). doi:10.1038/s41598-019-49444-y

7. Chen YL, Tuan HY, Tien CW, Lo WH, Liang HC, Hu YC. Augmented biosynthesis of cadmium sulfide nanoparticles by genetically engineered escherichia coli. *Biotechnol Prog*. 2009;25(5):1260-1266. doi:10.1002/btpr.199

8. Yuan Q, Bomma M, Xiao Z. Enhanced silver nanoparticle synthesis by escherichia coli transformed with candida albicans metallothionein gene. *Materials*. 2019;12(24). doi:10.3390/MA12244180

9. Yuan Q, Bomma M, Hill H, Xiao Z. Expression of Rhizobium tropici phytochelatin synthase in Escherichia coli resulted in increased bacterial selenium nanoparticle synthesis. *Journal of Nanoparticle Research*. 2020;22(12). doi:10.1007/s11051-020-05095-z

10. Choi Y, Lee SY. Biosynthesis of inorganic nanomaterials using microbial cells and bacteriophages. *Nat Rev Chem*. 2020;4(12):638-656. doi:10.1038/s41570-020-00221-w

11. Yoon J, Shin M, Lim J, Kim DY, Lee T, Choi JW. Nanobiohybrid Material-Based Bioelectronic Devices. *Biotechnol J*. 2020;15(6). doi:10.1002/biot.201900347

12. Choi Y, Park TJ, Lee DC, Lee SY. Recombinant Escherichia coli as a biofactory for various single- and multi-element nanomaterials. *Proc Natl Acad Sci U S A*. 2018;115(23):5944-5949. doi:10.1073/pnas.1804543115

13. Kang SH, Bozhilov KN, Myung N V., Mulchandani A, Chen W. Microbial synthesis of CdS nanocrystals in genetically engineered E. coli. *Angewandte Chemie - International Edition*. 2008;47(28):5186-5189. doi:10.1002/anie.200705806

14. Monrás JP, Díaz V, Bravo D, et al. Enhanced Glutathione Content Allows the In Vivo Synthesis of Fluorescent CdTe Nanoparticles by Escherichia coli. *PLoS One*. 2012;7(11). doi:10.1371/journal.pone.0048657

15. Rubino FM. Toxicity of glutathione-binding metals: A review of targets and mechanisms. *Toxics*. 2015;3(1):20-62. doi:10.3390/toxics3010020

16. Alisik M, Neselioglu S, Erel O. A colorimetric method to measure oxidized, reduced and total glutathione levels in erythrocytes. *Journal of Laboratory Medicine*. Published online 2019. doi:10.1515/labmed-2019-0098

17. Sharma A, Kumar V, Kaur P, Thukral AK, Bhardwaj R. Phytochemical and elemental analysis of Brassica juncea L. leaves using GC-MS and SEM-EDX. *Res J Pharm Technol*. 1997;8(12):1662-1664. doi:10.5958/0974-360X.2015.00299.1

18. Hemashree T, Prasunna SG, Sakthiselvan P. Synthesis of Keratin Nanoparticle and Characterization using FTIR. *Res J Pharm Technol*. 2019;12(6):2664. doi:10.5958/0974-360x.2019.00445.1

19. Smirnova, G. V., & Oktyabrsky, O. N. (2005). Glutathione in bacteria. *Biochemistry. Biokhimiia*, *70*(11), 1199–1211. https://doi.org/10.1007/s10541-005-0248-3.

20. Alonso-Moraga A, Bocanegra A, Torres JM, L6pez-Barea J, Pueyo C. *Glutathione Status and Sensitivity to GSH-Reacting Compounds of Escherichia Coli Strains Deficient in Glutathione Metabolism and/or Catalase Activity*. Vol 73.; 1987.

21. Pophaly SD, Singh R, Pophaly SD, Kaushik JK, Tomar SK. Current status and emerging role of glutathione in food grade lactic acid bacteria. *Microb Cell Fact*. 2012;11. doi:10.1186/1475-2859-11-114

22. Jaishankar J, Srivastava P. Molecular basis of stationary phase survival and applications. *Front Microbiol*. 2017;8(OCT). doi:10.3389/fmicb.2017.02000

23. Kram KE, Finkel SE. Culture volume and vessel affect long-term survival, mutation frequency, and oxidative stress of Escherichia coli. *Appl Environ Microbiol*. 2014;80(5):1732-1738. doi:10.1128/AEM.03150-13

24. Zitka O, Skalickova S, Gumulec J, et al. Redox status expressed as GSH:GSSG ratio as a marker for oxidative stress in paediatric tumour patients. *Oncol Lett*. 2012;4(6):1247-1253. doi:10.3892/ol.2012.931

25. Oktyabrskii ON, Smirnova G V. Redox potential changes in bacterial cultures under stress conditions. *Microbiology (N Y)*. 2012;81(2):131-142. doi:10.1134/S0026261712020099

26. Widness JK, Enny DG, McFarlane-Connelly KS, Miedenbauer MT, Krauss TD, Weix DJ. *CdS Quantum Dots as Potent Photoreductants for Organic Chemistry Enabled by Auger Recombination*.

27. Designed Research; S BKCJ, Performed Research; S SCJ. Acetogenic bacteria utilize light-driven electrons as an energy source for autotrophic growth. 118(9). doi:10.1073/pnas.2020552118/-/DCSupplemental

28. Gao X, Liu X, Zhu Z, et al. Enhanced visible light photocatalytic performance of CdS sensitized TiO2 nanorod arrays decorated with Au nanoparticles as electron sinks. *Sci Rep*. 2017;7(1). doi:10.1038/s41598-017-01124-5

29. Kaur J, Komal, Renu, et al. Glutathione Modified Fluorescent CdS QDs Synthesized Using Environmentally Benign Pathway for Detection of Mercury Ions in Aqueous Phase. *J Fluoresc*. 2020;30(4):773-785. doi:10.1007/s10895-020-02545-8

30. Thangadurai P, Balaji S, Manoharan PT. Surface modification of CdS quantum dots using thiols - Structural and photophysical studies. *Nanotechnology*. 2008;19(43). doi:10.1088/0957-4484/19/43/435708

31. Cobb JS, Zai-Rose V, Correia JJ, Janorkar A V. FT-IR Spectroscopic Analysis of the Secondary Structures Present during the Desiccation Induced Aggregation of Elastin-Like Polypeptide on Silica. *ACS Omega*. 2020;5(14):8403-8413. doi:10.1021/acsomega.0c00271

32. Ji Y, Yang X, Ji Z, et al. DFT-Calculated IR Spectrum Amide I, II, and III Band Contributions of N-Methylacetamide Fine Components. *ACS Omega*. 2020;5(15):8572-8578. doi:10.1021/acsomega.9b04421

33. Nyamu SN, Ombaka L, Masika E, Ng'ang'a M. One-pot microwave-assisted synthesis of size-dependent l -glutathione-capped spherical silver nanoparticles suitable for materials with antibacterial properties . *J Interdiscip Nanomed*. 2019;4(3):86-94. doi:10.1002/jin2.62

34. Nakkeeran S, Fernando WGD, Siddiqui ZA. Plant growth promoting rhizobacteria formulations and its scope in commercialization for the management of pests and diseases. In: *PGPR: Biocontrol and Biofertilization*. Springer Netherlands; 2006:257-296. doi:10.1007/1-4020-4152-7_10

35. Yuan Q, Bomma M, Hill H, Xiao Z. Expression of Rhizobium tropici phytochelatin synthase in Escherichia coli resulted in increased bacterial selenium nanoparticle synthesis. *Journal of Nanoparticle Research*. 2020;22(12). doi:10.1007/s11051-020-05095-z

36. Al-Hussam AMA, Jassim SAJ. Synthesis, structure, and optical properties of CdS thin films nanoparticles prepared by chemical bath technique. *Journal of the Association of Arab Universities for Basic and Applied Sciences*. 2012;11(1):27-31. doi:10.1016/j.jaubas.2011.10.001

37. Rodriguez P, Muñoz-Aguirre N, San-Martín Martinez E, González de la Cruz G, Tomas SA, Zelaya Angel O. Synthesis and spectral properties of starch capped CdS nanoparticles in aqueous solution. *J Cryst Growth*. 2008;310(1):160-164. doi:10.1016/j.jcrysgro.2007.09.036

38. Dhage SR, Colorado HA, Hahn T. Morphological variations in cadmium sulfide nanocrystals without phase transformation. *Nanoscale Res Lett*. 2011;6:1-5. doi:10.1186/1556-276X-6-420

39. Chandra PP, Mukherjee A, Mitra P. Synthesis of Nanocrystalline CdS by SILAR and Their Characterization. *J Mater*. 2014;2014:1-6. doi:10.1155/2014/138163

40. Sankhla A, Sharma R, Yadav RS, Kashyap D, Kothari SL, Kachhwaha S. Biosynthesis and characterization of cadmium sulfide nanoparticles - An emphasis of zeta potential behavior due to capping. *Mater Chem Phys*. 2016;170:44-51. doi:10.1016/j.matchemphys.2015.12.017

41. Kouhestany RH, Azizi SN, Shakeri P, Rahmani S. Sensitive Determination of Cetirizine Using CdS Quantum dots as Oxidase Mimic-mediated Chemiluminescence of Sulfite. *International Current Pharmaceutical Journal*. 2016;5(7):59-62. doi:10.3329/icpj.v5i7.28037